Exact analytical solutions for a diffusion problem coupled with a precipitation-dissolution reaction and feedback of porosity change

Mohamed Hayek,[1] Georg Kosakowski,[1] and Sergey Churakov[1]

[1]   We present exact analytical solutions for a one-dimensional diffusion problem coupled with the precipitation-dissolution reaction $A_{(aq)} + B_{(aq)} \rightleftharpoons M_{(s)}$ and feedback of porosity change. The solutions are obtained in the form of traveling waves and describe spatial and temporal evolutions of solute concentration, porosity, and mineral distribution for a set of initial and boundary conditions. The form of the solutions limits the choice of admissible boundary conditions, which might be difficult to adapt in natural systems, and thus, the solutions are of limited use for such a system. The main application of the derived solutions is therefore the benchmarking of numerical reactive transport codes for systems with strong porosity change. To test the performance of numerical codes, numerical solutions obtained by using a global implicit finite volume technique are compared to the analytical solutions. Good agreement is obtained between the analytical solutions and the numerical solutions when a sufficient spatial discretization resolves the spatial concentration gradients at any time. In the limit of fast kinetics (local equilibrium), steep concentration fronts cannot be resolved in a numerical discretization schema.

1.   Introduction

[2]   Reactive transport simulations through porous media have been widely applied to model the geochemical evolution of environmental systems. Typical examples are contaminant and radionuclide transport away from disposal sites, groundwater remediation (reactive barriers), ore body formation, and oil reservoir stimulation. Of special interest are the systems where precipitation and dissolution of minerals cause significant porosity changes [*Amos and Mayer*, 2006; *Cussler*, 1982; *Cussler et al.*, 1983; *Gruber*, 1990; *Lichtner*, 1991; *Lichtner et al.*, 1986a, 1986b; *Ortoleva et al.*, 1987a, 1987b; *Steefel and Maher*, 2009; *Weare et al.*, 1976]. At the pore scale, the precipitation-dissolution reactions modify the pore geometry and effective pore radii, causing a change in effective transport properties of the media [*MacQuarries and Mayer*, 2005; *Saripalli et al.*, 2001; *Steefel and Maher*, 2009].

[3]   Ultimately, precipitation may lead to complete clogging of the pore space and a virtual halt of the transport [*Amos and Mayer*, 2006; *Trotignon et al.*, 2006, 2007]. *Noiriel et al.* [2004, 2007] studied experimentally the dissolution of a porous limestone core during CO_2-enriched water injection with periodic X-ray microtomography imaging. They found a change in the parameters of the porosity-permeability relationship during dissolution, which they related to changes in the pore structure. *Singurindy and Berkowitz* [2003a, 2003b] investigated concurrent precipitation and dissolution processes with linear flow experiments in laboratory columns. They found a complex pattern of spatial and temporal variations in pore space that was leading to changes in effective transport properties of the media.

[4]   Reactive transport simulations on the field scale using pore-scale description of solute transport and precipitation-dissolution reactions are not feasible because of enormous computational costs. Therefore, a continuum description of mass transport in porous media is applied. Contrary to the pore scale, where the chemical and physical variables describing the system are discontinuous as a consequence of the granular nature of rocks, the value of each chemical and physical variable in the continuum scale is locally averaged over some representative elementary volume (REV) [*Bear*, 1972].

[5]   For an accurate system description, the REV should be larger than typical mineral grain size and pore space heterogeneities. From the chemical point of view, the REV should also contain enough polymineral grains to represent chemical composition of the system and so admit the calculation of local thermodynamic equilibrium [*Lichtner*, 1996].

[6]   If the system under investigation is subjected to the constraints of local thermodynamic equilibrium, the grid-based modeling of fluid-rock interactions using the REV description are complicated by the occurrence of discontinuous changes or jumps in solute concentration caused by change in the stable phase ensemble and therefore the equilibrium concentration in the solution. For the grid-based methods the flux between nodes with different stable mineral ensembles will eventually depend on the discretization of the domain. Many approximate numerical models

[1]Laboratory for Waste Management, Paul Scherrer Institut, Villigen PSI, Switzerland.

describing the evolution of mineral reaction zone (the porosity change) have been presented in the literature [*Adler et al.*, 1998; *Burnol et al.*, 2006; *Charlet et al.*, 2007; *De Windt et al.*, 2006, 2007a, 2007b; *Gaucher et al.*, 2004; *Marty et al.*, 2009; *Savage et al.*, 2002; *Soler*, 2003; *Spiteri et al.*, 2007; *Steefel and Lichtner*, 1994, 1998; *Trotignon et al.*, 2006, 2007; *Vieillard et al.*, 2007]. The numerical approaches that are based on the use of a fixed grid of nodes and elements predict discretization-dependent values of porosity, precipitation rates, and eventually the clogging time because of their inability to describe subgrid pore space changes correctly. This was clearly demonstrated by *Marty et al.* [2009], who showed that rate of precipitation reactions and grid size in numerical algorithms affect clogging times at material interfaces in a diffusive transport regime. In this context, exact analytical solutions (if they exist) become a necessity to validate the numerical solutions.

[7] Derivation of analytical solutions for systems that include porosity change and chemical reactions is not trivial because of the nonlinear nature of mass transport equations describing such problems. The only analytical solutions of this class reported in the literature are applicable to simplified systems. *Lichtner et al.* [1986a] have used exact results from the work of *Helfferich and Katchalsky* [1970] to compare the steady state limit of finite difference calculations describing the interdiffusion of two reacting species. Further, *Lichtner et al.* [1986b] compared exact and numerical solutions to the moving boundary problem resulting from reversible heterogeneous reactions and aqueous diffusion in a porous medium. *Knabner et al.* [1995] and *van Duijn et al.* [1998] proposed a model for transport of solutes in a porous medium participating in a precipitation-dissolution reaction. In all these works the porosity, however, was assumed to be constant in space and time. Recently, *Lagneau and van der Lee* [2010] proposed an analytical solution based on Fourier series for a reactive transport model with feedback of porosity change. However, their analytical solution is valid only at the very beginning of the system evolution in the limit of small spatial porosity changes. Therefore, this analytical solution does not describe systems with strong porosity changes, which eventually lead to complete clogging of the pore space.

[8] In this work, we use the simplest equation method [*Kudryashov*, 2005a, 2005b] to solve analytically a one-dimensional diffusion-reaction equation for systems in which mineral precipitation-dissolution reactions cause arbitrary strong porosity changes. The solutions are obtained in the form of traveling waves and describe spatial and temporal evolutions of solute concentration, porosity, and mineral distribution for a set of initial and boundary conditions. The form of the solutions limits the choice of admissible boundary conditions, which might be difficult to adapt in natural systems, and thus, the solutions are of limited use for such systems. However, the available boundary conditions can be simulated in well-designed experimental setups. The main application of the derived solutions is obviously in benchmarking numerical reactive transport codes for systems with strong porosity change.

[9] This paper is organized as follows: First, we present the governing equations for the reactive transport system. We then explain the mathematical background and the method used to find exact solutions of the problem. Exact explicit solutions are then presented that describe precipitation and dissolution of minerals. Finally, we compare the analytical solutions with numerical results.

2. Mathematical Formulation of the Problem

[10] Consider a porous column of length L with porosity $\phi = \phi(x, t)$ consisting of an inert solid matrix in addition to a reactive mineral phase (solid) $M_{(s)}$ in equilibrium with two aqueous species $A_{(aq)}$ and $B_{(aq)}$. Then, the single chemical reaction that occurs in the system is

$$A_{(aq)} + B_{(aq)} \rightleftharpoons M_{(s)}. \tag{1}$$
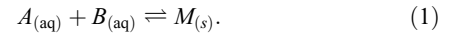
In order to simplify the derivation, we assume that the concentration of species B is fixed in space and maintained constant throughout the simulation time. This assumption limits the application to the natural system but does not lose generality for benchmarking numerical codes. Mathematically, the concentration profile of species B is defined by some arbitrary function $f(x)$ (see equation (6)).

[11] The partial differential equation determining the concentration of the aqueous component A is obtained from conservation of mass. Denoting the rate of the reaction given in (1) by $I(x, t)$, conservation of the aqueous species A is represented by

$$\frac{\partial(\phi c)}{\partial t} + \frac{\partial J}{\partial x} = I, \tag{2}$$

where $c = c(x, t)$ is the concentration of the species A (mol m^{-3}) and the flux J is given by Fick's law,

$$J = -D_e \frac{\partial c}{\partial x}, \tag{3}$$

where the effective diffusion coefficient D_e (m^2 s^{-1}) is assumed to be linearly proportional to the porosity (i.e., $D_e = D_0\phi$) with a constant pore diffusion coefficient D_0. This assumption is one of the possible relations between D_e and ϕ. More complex relations have been also reported in the literature [e.g., *Boving and Grathwohl*, 2001]. We limit ourselves to diffusive transport only, which is a dominant transport mechanism in systems with low hydraulic conductivity [*Desaulniers et al.*, 1981; *Johnson et al.*, 1989; *Shackelford and Daniel*, 1991; *Liu and Ball*, 1998; *Navarro et al.*, 2000; *Jang and Kim*, 2003; *Landais*, 2004].

[12] Conservation of the solid phase $M_{(s)}$ requires that the porosity satisfies

$$\frac{\partial\phi}{\partial t} = V_m I, \tag{4}$$

where V_m denotes the mineral (solid) molar volume (m^3 mol^{-1}). Since the system contains two aqueous species and one mineral and because the concentration of species B is fixed, the change in the volume of the solid phase is due to the change in the concentration of species A. This change in volume can be described by

$$\phi(x, t) = \phi_0(x) + V_m\phi_0(x)\bar{c}_0(x) - V_m\phi(x, t)\bar{c}(x, t), \tag{5}$$

where $\bar{c} = \bar{c}(x, t)$ denotes the concentration of the mineral phase (mol m^{-3} of fluid) and $\phi_0(x)$ and $\bar{c}_0(x)$ are the initial distributions of the porosity and the mineral concentration, respectively. In order to close the system of equations, the growth of mineral phase $M_{(s)}$ is simulated with the kinetic law

$$\frac{\partial(\phi\bar{c})}{\partial t} = -kS\left[1 - \frac{f(x)c}{K}\right], \tag{6}$$

where K is the solubility constant of the mineral (mol m^{-3}), k is the kinetic rate constant (mol m^{-2} s^{-1}) and $S = S(x, t)$ is the reactive surface area of the solid (m^2 m^{-3}). We assume a linear dependency, i.e., $S = S_0\phi$, where S_0 is a constant representing the specific surface area. In different systems, more complicated relationships can be found [e.g., *Noiriel et al.*, 2004, 2007; *Saripalli et al.*, 2001]. Equation (6) shows that the product $f(x)c$ determines the precipitation-dissolution rate, where $f(x)$ is the concentration of species B in reaction (1). By combining equations (2)–(6) we obtain a system of three partial differential equations with three unknowns, c, ϕ, and $\bar{c}$:

$$\frac{\partial(\phi c)}{\partial t} - \frac{\partial}{\partial x}\left(D_0\phi\frac{\partial c}{\partial x}\right) - \frac{1}{V_m}\frac{\partial\phi}{\partial t} = 0,$$

$$\frac{\partial\phi}{\partial t} = kV_mS_0\phi\left[1 - \frac{f(x)c}{K}\right], \tag{7}$$

$$\frac{\partial(\phi\bar{c})}{\partial t} = -\frac{1}{V_m}\frac{\partial\phi}{\partial t}.$$

The system of equations (7) describes a coupled diffusion-reaction problem with feedback of porosity change due to the precipitation-dissolution reaction (1). To solve the problem, initial and boundary conditions should be specified. The boundary conditions are of the form

$$c(0, t) = c_0(t), \quad t > 0, \tag{8}$$

$$c(L, t) = c_L(t), \quad t > 0, \tag{9}$$

where $c_0(t)$ and $c_L(t)$ are two functions of t.

[13] The initial conditions for the species concentration is defined as

$$c(x, 0) = c_i(x), \quad x \in [0, L], \tag{10}$$

where $c_i(x)$ is a function of x.

[14] The initial porosity and mineral concentration are assumed to be known:

$$\phi(x, 0) = \phi_0(x), \quad x \in [0, L], \tag{11}$$

$$\bar{c}(x, 0) = \bar{c}_0(x), \quad x \in [0, L]. \tag{12}$$

In the following, we derive exact analytical solutions for system (7) with the boundary and initial conditions (8)–(12).

3. Methodology

[15] In this section, we describe the methodology used to find exact solutions for system (7). The idea is to convert the system of nonlinear partial differential equations (7) to a system of nonlinear ordinary differential equations (NODEs) by making some transformations. Then the NODEs can be solved through the simplest equation method. In order to obtain a system of NODEs from the nonlinear system of partial differential equations (7), we introduce the transformation

$$\xi = \int \sigma(x)dx - \lambda t, \tag{13}$$

where $\sigma(x)$ is a function that depends on the space coordinate x, to be determined later, and λ is an arbitrary constant. Transformation (13) allows us to work with one variable, ξ, instead of the two variables, x and t. Therefore, we define

$$c(x, t) = C(\xi), \phi(x, t) = \Phi(\xi), \bar{c}(x, t) = \bar{C}(\xi). \tag{14}$$

In (14), we use $C(\xi)$, $\Phi(\xi)$, and $\bar{C}(\xi)$ rather than $c(\xi)$, $\phi(\xi)$, and $\bar{c}(\xi)$ to avoid any nomenclature confusion. Using transformation (13), we can easily obtain the following relationships between the partial differential operators $\partial/\partial t$, $\partial/\partial x$, and $\partial^2/\partial x^2$ and the ordinary differential operators $d/d\xi$ and $d^2/d\xi^2$

$$\frac{\partial}{\partial t} = -\lambda\frac{d}{d\xi}, \frac{\partial}{\partial x} = \sigma(x)\frac{d}{d\xi},$$

$$\frac{\partial^2}{\partial x^2} = \sigma'(x)\frac{d}{d\xi} + \sigma^2(x)\frac{d^2}{d\xi^2}, \tag{15}$$

where $\sigma'(x)$ is the derivative of $\sigma(x)$ with respect to the space variable x. According to these relationships, system of equations (7) becomes the following system of NODEs:

$$\lambda\frac{d(\Phi C)}{d\xi} + D_0\sigma^2(x)\frac{d\Phi}{d\xi}\frac{dC}{d\xi} + D_0\Phi\left[\sigma'(x)\frac{dC}{d\xi} + \sigma^2(x)\frac{d^2C}{d\xi^2}\right]$$

$$- \frac{\lambda}{V_m}\frac{d\Phi}{d\xi} = 0,$$

$$\lambda\frac{d\Phi}{d\xi} = -kV_mS_0\Phi\left[1 - \frac{f(x)C}{K}\right], \tag{16}$$

$$\frac{d(\Phi\bar{C})}{d\xi} = -\frac{1}{V_m}\frac{d\Phi}{d\xi}.$$

It is important to mention that ξ is the dependent variable in system of equations (16), whereas x is independent of ξ. Substituting the second equation of system (16) into the first one, we obtain

$$\lambda\Phi\frac{dC}{d\xi} + D_0\Phi\left[\sigma'(x)\frac{dC}{d\xi} + \sigma^2(x)\frac{d^2C}{d\xi^2}\right] + D_0\sigma^2(x)\frac{d\Phi}{d\xi}\frac{dC}{d\xi}$$

$$+ kV_mS_0\Phi\left(\frac{1}{V_m} - C\right)\left[1 - \frac{f(x)C}{K}\right] = 0. \tag{17}$$

Equation (17) is a NODE that relates the two unknowns C and Φ. To solve this equation, we should eliminate one of these two unknowns from the equation. The easiest way is to eliminate Φ by making use of the second equation of

system (16). Indeed, from the second equation of system (16) we get

$$\frac{d\Phi}{d\xi} = -\frac{kV_mS_0}{\lambda}\Phi\left[1 - \frac{f(x)C}{K}\right]. \tag{18}$$

Therefore, substituting equation (18) into the third term of equation (17) and further manipulating equation (17), we obtain the following nonlinear ordinary differential equation in C:

$$D_0\sigma^2(x)\frac{d^2C}{d\xi^2} + \left[\lambda + D_0\sigma'(x) - \frac{kV_mD_0S_0\sigma^2(x)}{\lambda}\right]\frac{dC}{d\xi}$$
$$+ \frac{kV_mD_0S_0\sigma^2(x)f(x)}{K\lambda}C\frac{dC}{d\xi} + \frac{kV_mS_0f(x)}{K}C^2 \tag{19}$$
$$- kS_0\left[V_m + \frac{f(x)}{K}\right]C + kS_0 = 0.$$

When an exact solution $C(\xi) = c(x,t)$ of equation (19) is found, $\Phi(\xi) = \phi(x,t)$ and $\bar{C}(\xi) = \bar{c}(x,t)$ can be easily determined from the second equation of system (16) and equation (5), respectively. Indeed, the second equation of this system is a first-order ordinary differential equation (ODE) in Φ, which is solved straightforwardly

$$\Phi(\xi) = \Phi_1\exp\left\{-\frac{kV_mS_0}{\lambda}\left[\xi - \xi_1 - \frac{f(x)}{K}\int_{\xi_1}^{\xi}C(\xi')d\xi'\right]\right\}, \tag{20}$$

where Φ_1 and ξ_1 are two arbitrary constants.

[16] The analytical expression of the mineral concentration can be obtained from equation (5). For simplicity, we neglect the mass fraction of the inert solid. In this case we have $\phi_0(x) + V_m\phi_0(x)\bar{c}_0(x) = 1$. Therefore, from equation (5) we get the analytical expression of the mineral concentration as follows:

$$\bar{c}(x,t) = \frac{1}{V_m}\left[\frac{1}{\phi(x,t)} - 1\right]. \tag{21}$$

[17] In section 4, equation (19) is solved using the simplest equation method. This method is a very powerful mathematical technique for finding exact solutions of nonlinear ordinary differential equations. It was developed by *Kudryashov* [2005a, 2005b] and has been used successfully by many authors for finding exact solutions of ODEs in mathematical physics [*Kudryashov and Loguinova*, 2008; *Vitanov et al.*, 2010; *Vitanov and Dimitrova*, 2010]. Further details can be found in Appendix A.

4. Exact Solutions of System (7)

[18] In order to find exact solutions of system (7), we first determine $C(\xi) = c(x,t)$ by solving equation (19). Knowing the solute concentration $c(x,t)$, we can calculate the porosity $\phi(x,t)$ and the mineral concentration $\bar{c}(x,t)$ by using equations (20) and (21), respectively. Details of the derivation of the porosity functions are given in Appendix B.

[19] We apply now the simplest equation method to equation (19) in order to find exact solutions of the solute concentration $c(x,t) = C(\xi)$. Therefore, we assume that the solute concentration can be written as finite series (A2) of the solutions of the simplest equation. The Bernoulli equation (A3) is used as the simplest equation. The parameter N in equation (A2) is determined by inserting equation (A3) into equation (19) and balancing the high-order linear term with the high-order nonlinear term. Then, we balance $d^2C/d\xi^2$ with $C(dC/d\xi)$, and we obtain $N + 2 = N + N + 1$, so that $N = 1$. Therefore, the exact solutions of equation (19) can be written as

$$C(\xi) = A_0(x) + A_1(x)Y, \quad A_1(x) \neq 0, \tag{22}$$

where $A_0(x)$ and $A_1(x)$ are two functions to be determined and ξ is defined by (13). Since the coefficients of equation (19) depend on x, we assume that the coefficients A_0 and A_1 in equation (22) and the coefficients a and b of the Bernoulli equation (A3) also depend on x. Substituting (22) into (19) along with (A3), we obtain a polynomial in Y. Vanishing all the coefficients of this polynomial yields the following system of overdetermined differential equations of $\sigma(x)$, $a(x)$, $b(x)$, $A_0(x)$, and $A_1(x)$:

$$kS_0[V_mA_0(x) - 1][f(x)A_0(x) - K] = 0,$$

$$A_1(x)\{kV_mD_0S_0a(x)\sigma^2(x)[f(x)A_0(x) - K] + kS_0\lambda[2V_mf(x)A_0(x)$$
$$- KV_m - f(x)] + \lambda Ka(x)[\lambda + D_0a(x)\sigma^2(x) + D_0\sigma'(x)]\} = 0,$$

$$A_1(x)\{kV_mD_0S_0b(x)\sigma^2(x)[f(x)A_0(x) - K] + kS_0V_mf(x)A_1(x)$$
$$\cdot[D_0a(x)\sigma^2(x) + \lambda] + \lambda Kb(x)[\lambda + 3D_0a(x)\sigma^2(x) + D_0\sigma'(x)]\} = 0,$$

$$D_0A_1(x)b(x)\sigma^2(x)[2\lambda Kb(x) + kV_mS_0A_1(x)f(x)] = 0.$$
$$\tag{23}$$

This system can be solved analytically with the help of packages for computer algebra like Maple and Mathematica. Solving system (23) leads to the following five exact solutions of the system:

S_1

$$\sigma(x) = C_1, \quad a(x) = -\frac{\lambda}{D_0C_1^2}, \, b(x) = 0, \quad A_0(x) = \frac{1}{V_m},$$
$$A_1(x) = A_1(x);$$

S_2

$$\sigma(x) = 0, \quad a(x) = -\frac{kS_0[f(x) - KV_m]}{\lambda K}, \quad b(x) = b(x),$$
$$A_0(x) = \frac{K}{f(x)}, \quad A_1(x) = -\frac{\lambda Kb(x)}{kS_0V_mf(x)};$$

S_3

$$\sigma(x) = 0, \quad a(x) = -\frac{kS_0[f(x) - KV_m]}{\lambda K}, \quad b(x) = b(x),$$
$$A_0(x) = \frac{1}{V_m}, \quad A_1(x) = -\frac{\lambda Kb(x)}{kS_0V_mf(x)};$$

S_4

$$\sigma'(x) = \frac{\lambda}{D_0} - \frac{kS_0[f(x) - KV_m]}{2\lambda K}\sigma^2(x), \quad a(x) = \frac{kS_0[f(x) - KV_m]}{2\lambda K},$$

$$b(x) = b(x), \quad A_0(x) = \frac{K}{f(x)}, \quad A_1(x) = -\frac{2\lambda Kb(x)}{kS_0 V_m f(x)};$$

S_5

$$\sigma'(x) = \frac{\lambda}{D_0} - \frac{kS_0[f(x) - KV_m]}{2\lambda K}\sigma^2(x), \quad a(x) = -\frac{kS_0[f(x) - KV_m]}{2\lambda K},$$

$$b(x) = b(x), \quad A_0(x) = \frac{1}{V_m}, \quad A_1(x) = -\frac{2\lambda Kb(x)}{kS_0 V_m f(x)},$$

where C_1 is a constant of integration.

[20] Each solution of system (23) will give analytical solutions of the system (7) as described in sections 4.1–4.2.

4.1. Analytical Solutions Derived From S_1

[21] Since $b(x) = 0$ in S_1, we use solution (A5) of the Bernoulli equation. Substituting (A5) into (22) and using S_1, we obtain the following analytical solution of the solute concentration

$$c(x,t) = \frac{1}{V_m} + A_1(x)\exp\left[-\frac{\lambda(C_1 x - \lambda t + C_1 x_0 + \xi_0)}{D_0 C_1^2}\right], \quad (24)$$

where x_0 is a constant of integration. The function $A_1(x)$ in (24) is an arbitrary function that depends on the space variable x. It is related to the initial condition $c_i(x) = c(x, 0)$ by

$$A_1(x) = \left[c_i(x) - \frac{1}{V_m}\right]\exp\left[\frac{\lambda(C_1 x + C_1 x_0 + \xi_0)}{D_0 C_1^2}\right]. \quad (25)$$

One of the functions $A_1(x)$ or $c_i(x)$ has to be defined. If we define the initial condition, then $A_1(x)$ is calculated by (25), and the analytical solution of the solute concentration becomes

$$c(x,t) = \frac{1}{V_m} + \left[c_i(x) - \frac{1}{V_m}\right]\exp\left(\frac{\lambda^2 t}{D_0 C_1^2}\right). \quad (26)$$

[22] In this case, the boundary conditions $c_0(t) = c(0, t)$ and $c_L(t) = c(L, t)$ are simply calculated by substituting x by 0 and L in (26), respectively:

$$c_0(t) = \frac{1}{V_m} + \left[c_i(0) - \frac{1}{V_m}\right]\exp\left(\frac{\lambda^2 t}{D_0 C_1^2}\right), \quad (27)$$

$$c_L(t) = \frac{1}{V_m} + \left[c_i(L) - \frac{1}{V_m}\right]\exp\left(\frac{\lambda^2 t}{D_0 C_1^2}\right). \quad (28)$$

The analytical solution of the porosity is obtained by substituting S_1 along with (25) into (B5):

$$\phi(x,t) = \Phi_1 \exp\left\{\frac{kS_0[f(x) - KV_m](C_1 x - \lambda t + C_1 x_0 - \xi_1)}{\lambda K}\right\}$$

$$\cdot \exp\left(\frac{kS_0 D_0 C_1^2 f(x)[1 - V_m c_i(x)]}{\lambda^2 K}\left\{\exp\left(\frac{\lambda^2 t}{D_0 C_1^2}\right)\right.\right. \quad (29)$$

$$\left.\left. - \exp\left[\frac{\lambda(C_1 x + C_1 x_0 - \xi_1)}{D_0 C_1^2}\right]\right\}\right).$$

Substituting (29) into (21), we get the following analytical solution for the mineral concentration:

$$\bar{c}(x,t) = \frac{1}{\Phi_1 V_m}\exp\left\{\frac{kS_0[KV_m - f(x)](C_1 x - \lambda t + C_1 x_0 - \xi_1)}{\lambda K}\right\}$$

$$\cdot \exp\left(\frac{kS_0 D_0 C_1^2 f(x)[V_m c_i(x) - 1]}{\lambda^2 K}\left\{\exp\left(\frac{\lambda^2 t}{D_0 C_1^2}\right)\right.\right.$$

$$\left.\left. - \exp\left[\frac{\lambda(C_1 x + C_1 x_0 - \xi_1)}{D_0 C_1^2}\right]\right\}\right) - \frac{1}{V_m}. \quad (30)$$

4.2. Analytical Solutions Derived From S_2

[23] We assume that $b(x) \neq 0$ in S_2. Therefore, in (22), Y is defined by (A4). By using the solution S_2 of system (23) we obtain the following analytical solution of the solute concentration:

$$c(x,t) = \frac{KV_m - b(x)f(x)\exp\left\{\frac{kS_0[f(x) - KV_m](x_0 + \xi_0 - \lambda t)}{\lambda K}\right\}}{V_m f(x)\left(1 - b(x)\exp\left\{\frac{kS_0[f(x) - KV_m](x_0 + \xi_0 - \lambda t)}{\lambda K}\right\}\right)}, \quad (31)$$

where x_0 is a constant of integration and $b(x)$ can be calculated from the initial concentration,

$$b(x) = \frac{V_m[f(x)c_i(x) - K]}{f(x)[V_m c_i(x) - 1]}\exp\left\{-\frac{kS_0[f(x) - KV_m](x_0 + \xi_0)}{\lambda K}\right\}. \quad (32)$$

Substituting (32) into (31), the analytical solution of the solute concentration can be written as a function of the initial concentration:

$$c(x,t) =$$

$$\frac{K[V_m c_i(x) - 1] - [f(x)c_i(x) - K]\exp\left\{-\frac{kS_0[f(x) - KV_m]t}{K}\right\}}{f(x)[V_m c_i(x) - 1] - V_m[f(x)c_i(x) - K]\exp\left\{-\frac{kS_0[f(x) - KV_m]t}{K}\right\}}. \quad (33)$$

[24] Solution (33) is subject to the following boundary conditions at $x = 0$ and $x = l$, respectively:

$$c_0(t) =$$

$$\frac{K[V_m c_i(0) - 1] - [f(0)c_i(0) - K]\exp\left\{-\frac{kS_0[f(0) - KV_m]t}{K}\right\}}{f(0)[V_m c_i(0) - 1] - V_m[f(0)c_i(0) - K]\exp\left\{-\frac{kS_0[f(0) - KV_m]t}{K}\right\}}, \quad (34)$$

$$c_L(t) =$$

$$\frac{K[V_m c_i(L) - 1] - [f(L)c_i(L) - K]\exp\left\{-\frac{kS_0[f(L) - KV_m]t}{K}\right\}}{f(L)[V_m c_i(L) - 1] - V_m[f(L)c_i(L) - K]\exp\left\{-\frac{kS_0[f(L) - KV_m]t}{K}\right\}}. \quad (35)$$

We use the solution (B3) for the porosity since $b(x) \neq 0$. Therefore, by substituting S_2 into (B3) we get the analytical solution of the porosity as follows:

$$\phi(x,t) = \Phi_1 \left| \frac{f(x)[V_m c_i(x) - 1] - V_m[f(x)c_i(x) - K] \exp\left\{-\dfrac{kS_0[f(x) - KV_m]t}{K}\right\}}{f(x)[V_m c_i(x) - 1] - V_m[f(x)c_i(x) - K] \exp\left\{\dfrac{kS_0[f(x) - KV_m](\xi_1 - x_0)}{\lambda K}\right\}} \right|. \tag{36}$$

The following analytical solution of the mineral concentration is obtained by substituting (36) into (21):

$$\bar{c}(x,t) = \frac{1}{\Phi_1 V_m} \left| \frac{f(x)[V_m c_i(x) - 1] - V_m[f(x)c_i(x) - K] \exp\left\{\dfrac{kS_0[f(x) - KV_m](\xi_1 - x_0)}{\lambda K}\right\}}{f(x)[V_m c_i(x) - 1] - V_m[f(x)c_i(x) - K] \exp\left\{-\dfrac{kS_0[f(x) - KV_m]t}{K}\right\}} \right| - \frac{1}{V_m}. \tag{37}$$

4.3. Analytical Solutions Derived From S_3

[25] If we assume in S_3 that $b(x)$ is a known function such that $b(x) \neq 0$, then by using solution (A4) of the Bernoulli equation in (22) we get the analytical solution of the solute concentration:

$$c(x,t) = \frac{f(x) - KV_m b(x) \exp\left\{-\dfrac{kS_0[f(x) - KV_m](x_0 + \xi_0 - \lambda t)}{\lambda K}\right\}}{V_m f(x) \left(1 - b(x) \exp\left\{-\dfrac{kS_0[f(x) - KV_m](x_0 + \xi_0 - \lambda t)}{\lambda K}\right\}\right)}, \tag{38}$$

where x_0 is a constant of integration and $b(x)$ can be calculated from the initial concentration,

$$b(x) = \frac{f(x)[V_m c_i(x) - 1]}{V_m[f(x)c_i(x) - K]} \exp\left\{\frac{kS_0[f(x) - KV_m](x_0 + \xi_0)}{\lambda K}\right\}. \tag{39}$$

[26] Substituting (39) into (38), the analytical solution of the solute concentration can be written as function of the initial concentration:

$c(x,t)$

$$= \frac{f(x)c_i(x) - K - K[V_m c_i(x) - 1] \exp\left\{\dfrac{kS_0[f(x) - KV_m]t}{K}\right\}}{V_m[f(x)c_i(x) - K] - f(x)[V_m c_i(x) - 1] \exp\left\{\dfrac{kS_0[f(x) - KV_m]t}{K}\right\}}. \tag{40}$$

The corresponding boundary conditions are defined by

$c_0(t)$

$$= \frac{f(0)c_i(0) - K - K[V_m c_i(0) - 1] \exp\left\{\dfrac{kS_0[f(0) - KV_m]t}{K}\right\}}{V_m[f(0)c_i(0) - K] - f(0)[V_m c_i(0) - 1] \exp\left\{\dfrac{kS_0[f(0) - KV_m]t}{K}\right\}}, \tag{41}$$

$c_L(t)$

$$= \frac{f(L)c_i(L) - K - K[V_m c_i(L) - 1] \exp\left\{\dfrac{kS_0[f(L) - KV_m]t}{K}\right\}}{V_m[f(L)c_i(L) - K] - f(L)[V_m c_i(L) - 1] \exp\left\{\dfrac{kS_0[f(L) - KV_m]t}{K}\right\}}. \tag{42}$$

After substituting solution S_3 into (B3), we get the following analytical solution of the porosity:

$$\phi(x,t) = \Phi_1 \exp\left\{-\frac{kS_0[KV_m - f(x)](x_0 - \lambda t - \xi_1)}{\lambda K}\right\} \left| \frac{V_m[f(x)c_i(x) - K] - f(x)[V_m c_i(x) - 1] \exp\left\{\dfrac{kS_0[f(x) - KV_m]t}{K}\right\}}{V_m[f(x)c_i(x) - K] - f(x)[V_m c_i(x) - 1] \exp\left\{-\dfrac{kS_0[f(x) - KV_m](\xi_1 - x_0)}{K}\right\}} \right|. \tag{43}$$

We arrive at the following analytical solution of the solid concentration by substituting (43) into (21):

$$\bar{c}(x,t) = \frac{1}{\Phi_1 V_m} \exp\left\{\frac{kS_0[KV_m - f(x)](x_0 - \lambda t - \xi_1)}{\lambda K}\right\} \left| \frac{V_m[f(x)c_i(x) - K] - f(x)(V_mc_i(x) - 1)\exp\left\{-\dfrac{kS_0[f(x) - KV_m](\xi_1 - x_0)}{K}\right\}}{V_m[f(x)c_i(x) - K] - f(x)[V_mc_i(x) - 1]\exp\left\{\dfrac{kS_0[f(x) - KV_m]t}{K}\right\}} \right| - \frac{1}{V_m}.$$

(44)

4.4. Analytical Solutions Derived From S_4 and S_5

[27] To obtain exact solutions from S_4 and S_5, we need to solve the Riccati equation with variable coefficients verified by $\sigma(x)$:

$$\sigma'(x) = \frac{\lambda}{D_0} - \frac{kS_0[f(x) - KV_m]}{2\lambda K}\sigma^2(x).$$

(45)

The solutions of the Riccati equation (45) depend on the function $f(x)$. This equation cannot be solved analytically for an arbitrary function $f(x)$. However, exact solutions can be obtained for special forms of $f(x)$ (see *Polyanin and Zaitsev* [2003] for further details).

5. Applications and Validations

[28] To illustrate the exact solutions, we present two examples for one-dimensional systems involving transport of one solute species through a saturated porous column. The second solute species in reaction (1) is fixed in space and maintained constant in time. Such conditions can be reproduced in principle in a controlled experiment by buffering the concentration of species B. Without loss of generality, we consider two examples describing the precipitation and dissolution of two hypothetical minerals. The first example is based on precipitation of minerals, which induces a porosity decrease. This example reaches clogging, i.e., complete filling of the pore space with precipitate. The second example represents the dissolution of minerals. Contrary to the first example, dissolution results in a porosity increase. The molar volume of minerals was set to unity. The solubility constants for minerals were taken from the general thermodynamic database THERMODDEM [*Piantone at al.*, 2006].

5.1. Precipitation of Minerals

[29] We assume that the concentration of species B is fixed, and it is represented by $f(x)$. Therefore, $c(x, t)$ represents the concentration of species A. For this example, we calculate solute concentration, porosity, and solid concentration using solutions derived from S_1 (i.e., solutions (26), (29), and (30), respectively).

[30] The aim of this example is to simulate the porosity evolution in a truly clogging system. To facilitate the analysis, we assume $f(x)$ to be constant and equal to 1. Therefore, precipitation of minerals occurs only if $c(x,t) > K$. The initial concentration of species A is defined by

$$c_i(x) = c(x,0) = \frac{1}{V_m} + \alpha \exp\left(-\frac{\lambda x}{D_0 C_1}\right),$$

(46)

where α is some arbitrary constant. Therefore, the solute concentration (26) is simplified to

$$c(x,t) = \frac{1}{V_m} + \alpha \exp\left[-\frac{\lambda(C_1 x - \lambda t)}{D_0 C_1^2}\right].$$

(47)

It is clear that if $\alpha > 0$, then the molar volume should take a large value in order to insure reasonable values of concentrations. The value of the molar volume was set to unity, which is highly unrealistic; however, this value does not prevent the applicability of this example for benchmarking numerical codes. The values of system parameters are given in Table 1. These parameters are selected in such a way that the concentrations are in realistic physical and chemical ranges (nonnegative values and maximal concentrations are of the order of 10^3 mol m^{-3}).

[31] We show in Figure 1 the solute concentration for successive times. As we see in Figure 1, the solute concentration increases with time at the left boundary and remains constant at the right boundary. Moreover, we always have $c(x,t) > K$. Consequently, we would expect a significant decrease of porosity at the left boundary.

[32] The porosity evolution with time is plotted in Figure 2. As expected, the porosity decreases significantly with time at the left boundary. We observe also a minor decrease of the porosity at the right boundary. This is because $c(x,t) > K$ and the solute concentration does not vary much at this boundary. The porosity continues to decrease and reaches very small values (near clogging). In numerical codes, a minimal porosity ϕ_m is defined, and clogging

Table 1. System Parameters of the Precipitation and Dissolution Examples

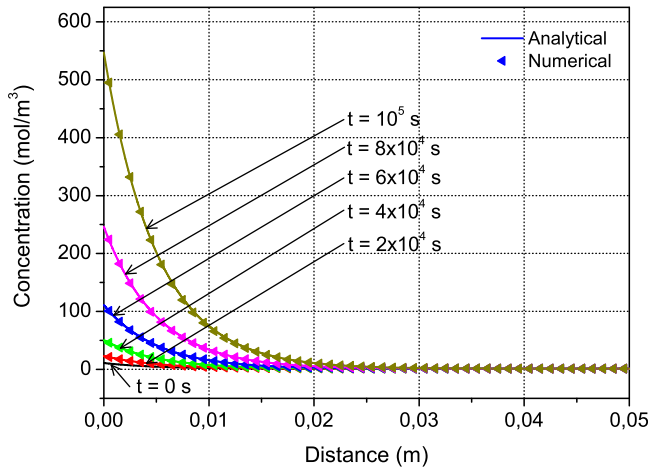| Parameter	Value	
	Precipitation Example	Dissolution Example
D_0 (m^2 s^{-1})	10^{-9}	10^{-11}
Φ_1	0.2	0.5
$\log(K)$	-0.16	-10.05
k (mol m^{-2} s^{-1})	10^{-10}	6×10^{-10}
V_m (m^3 mol^{-1})	1.0	1.0
S_0 (m^2 m^{-3})	5×10^3	3×10^4
C_1	1.0	–
α	10.0	10^3
β	–	0.1
λ	2×10^{-7}	–
μ	–	10^{-2}
γ	–	-5×10^3
θ	–	0.2
x_0	0	0
ξ_1	0	0

Figure 1. The analytical and numerical concentration profiles of species A for successive times for the example of mineral precipitation.

occurs once the porosity reaches this value. Our analytical solution allows us to define a theoretical clogging time, which is the time when the porosity reaches the minimal porosity ϕ_m. Taking into account $x_0 = \xi_1 = 0$, the porosity function (29) can be simplified to

$$\phi(x,t) = \Phi_1 \exp\left(\frac{kS_0(1 - KV_m)(C_1 x - \lambda t)}{\lambda K}\right. \\ \left. - \frac{\alpha k S_0 V_m D_0 C_1^2}{\lambda^2 K}\left\{\exp\left[-\frac{\lambda(C_1 x - \lambda t)}{D_0 C_1^2}\right] - 1\right\}\right). \quad (48)$$

From (48) we derive the time necessary to clog the system at the location x as

$$t_c(x) = \frac{1}{\lambda^2}[\lambda C_1 x + \lambda^2 \Theta - D_0 C_1^2 W(\Theta)], \quad (49)$$

where Θ is defined by

$$\Theta = \frac{\alpha k S_0 V_m D_0 C_1^2 - \lambda^2 K[\ln(\phi_m) - \ln(\Phi_1)]}{\lambda^2 k S_0 (1 - KV_m)} \quad (50)$$
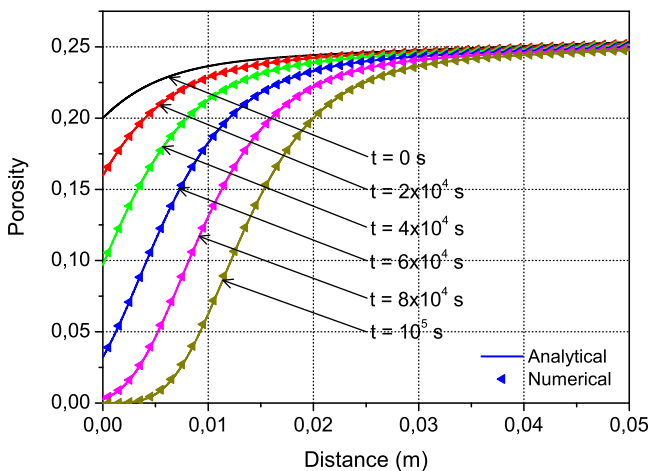
and W is the Lambert W function.

Figure 2. The analytical and numerical porosity profiles for successive times for the example of mineral precipitation.
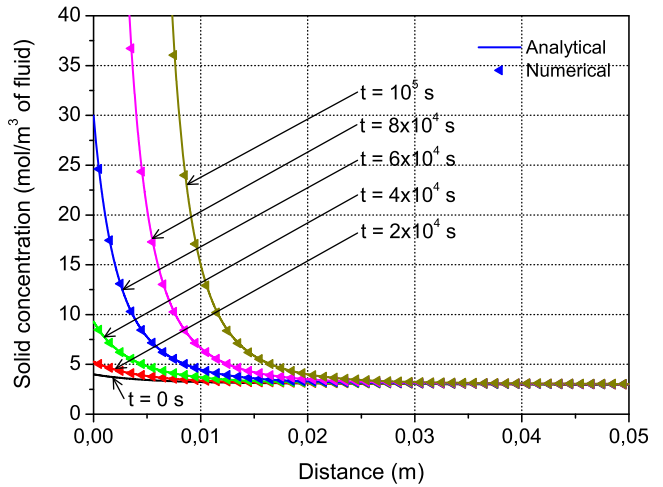

Figure 3. The analytical and numerical solid phase concentration profiles in moles per cubic meter of fluid for successive times for the example of mineral precipitation.

[33] Evolutions of the mineral concentration in moles per cubic meter of fluid $\bar{c}(x,t)$ for successive times are plotted in Figure 3. The decrease of porosity is due to the precipitation of minerals. Consequently, the precipitation of minerals occurs at the left boundary of the domain, as we can observe in Figure 3. Solid concentrations depend on the amount of liquid in the system. That means that if the porosity decreases toward zero, as we can deduce from equation (21), the solid concentration (defined in units of mol m^{-3} of fluid) goes to infinity, although the absolute solid amount is nearly constant. The concentration of the solid phase in moles per cubic meter of rock $\bar{C} = \phi\bar{c}$ is plotted in Figure 4. Contrary to $\bar{c}$, which tends to infinity as the porosity tends to zero, the amount $\bar{C}$ tends to a constant value when the porosity goes to zero (here $\bar{C} = 10^3$). The quantity $\bar{C}$ can only change if the mineral precipitates and does not depend on porosity. On the contrary, $\bar{c}$ evolves with mineral reactions and with porosity changes. Finally, one can see that although the clogging is reached at the left boundary, the precipitation of minerals continues in the
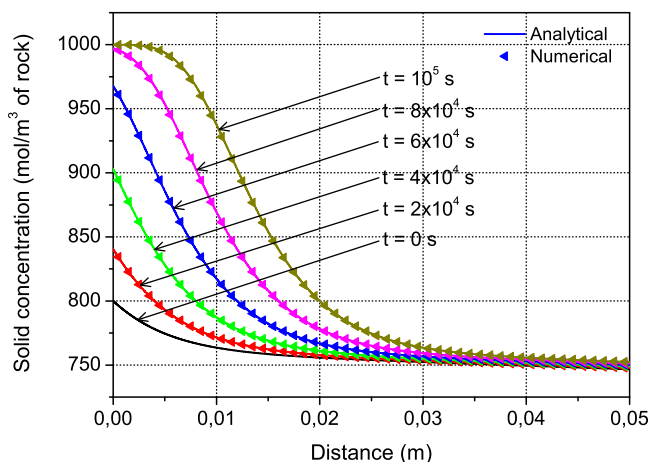

Figure 4. The analytical and numerical solid phase concentration profiles in moles per cubic meter of rock for successive times for the example of mineral precipitation.

system. Indeed, the system is oversaturated after clogging, and precipitation in the right part of the system continues according to the kinetic law. In addition, solute flux over the left boundary goes down strongly but never reaches zero. This is because the concentration at the left boundary increases steadily, which partly counterbalances the clogging effect. Moreover, the constant pore diffusion coefficient D_0 increases this effect.

5.2. Dissolution of Minerals

[34] This example involves a single solid phase $M_{(s)}$ reacting with the solutes according to reaction (1). For this example, we calculate solute concentration, porosity, and solid concentration using solutions derived from S_2 (i.e., solutions (33), (36), and (37), respectively).

[35] In these solutions, $c(x, t)$ represents the concentration of species A, and $f(x)$ is the concentration of species B, which is fixed. In this example, the initial concentration $c_i(x)$ is defined by

$$c_i(x) = \theta \exp(-\alpha x), \quad (51)$$

and the function $f(x)$ is the following sigmoid function:

$$f(x) = \frac{\beta}{1 + \exp[\gamma(x - \mu)]}, \quad (52)$$

where α, β, γ, θ, and μ are parameters chosen in such a way that the values of $c_i(x)$ and $f(x)$ represent realistic concentration values. The parameters of the problem are presented in Table 1. As in the previous example, the molar volume is fixed to unity. The choice of this value allows a considerable change in the porosity. For smaller and more realistic values of the molar volume, either the concentrations have to be very high, or the porosity change has to be very small.

[36] In Figure 5, we show the function $f(x)$ and the concentration profiles of species A for successive times. The front of the function $f(x)$ is approximately located at $x_f = 10^{-2}$ m. As we observe, the concentration increases with time near the boundary (i.e., in the region $0 \leq x \leq x_f$).
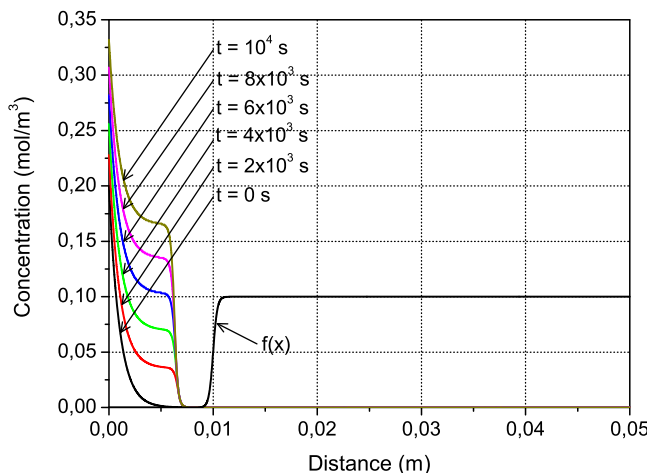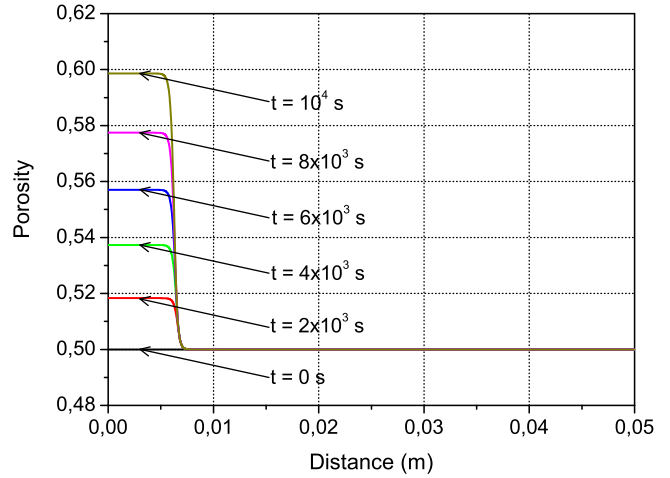

Figure 6. The analytical porosity profiles for successive times for the example of mineral dissolution.

Close to the boundary, the function $f(x)$ has very low values (i.e., of the order of 10^{-20}); therefore, the product $f(x)c(x, t)$ is dominated by the value of $f(x)$, and even the concentration of species A increases with time. Therefore, this product remains smaller than $K(\approx 10^{-10})$. Consequently, from the second equation of system (7), an increase in porosity is expected in the region near the boundary.

[37] Figure 6 shows the porosity profiles for several times. We observe a 5 mm wide region near the left boundary with constant porosity that increases with time. The value of the porosity in this region is practically constant at each time since the product $f(x)c(x, t)$ does not vary so much with time. The mineral concentration profiles are plotted in Figure 7 for various times, indicating dissolution of minerals near the boundary. We would like to mention that for long times, solute concentration values at the boundary become very high and the porosity can reach values larger than 1 (and, consequently, the mineral concentration becomes negative). Such unrealistic concentration values show the limited applicability of this analytical solution for real geochemical systems. This, however, does not hinder its application for benchmarking numerical codes.
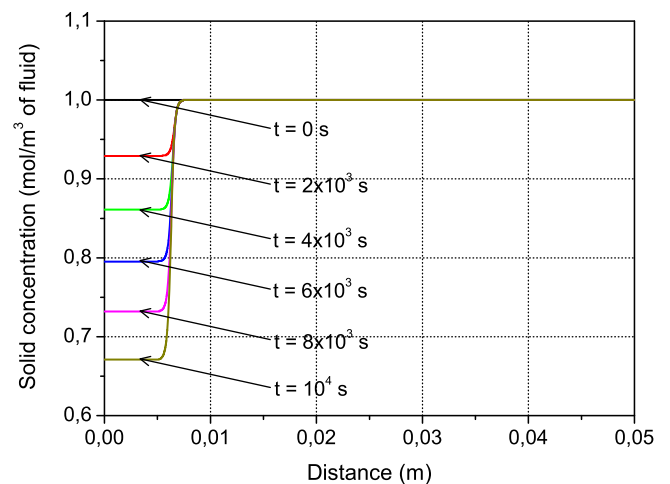

Figure 5. The shape of function $f(x)$ (concentration of species B) and the analytical concentration profiles of species A for successive times for the example of mineral dissolution.

Figure 7. The analytical solid phase concentration profiles for successive times for the example of mineral dissolution.
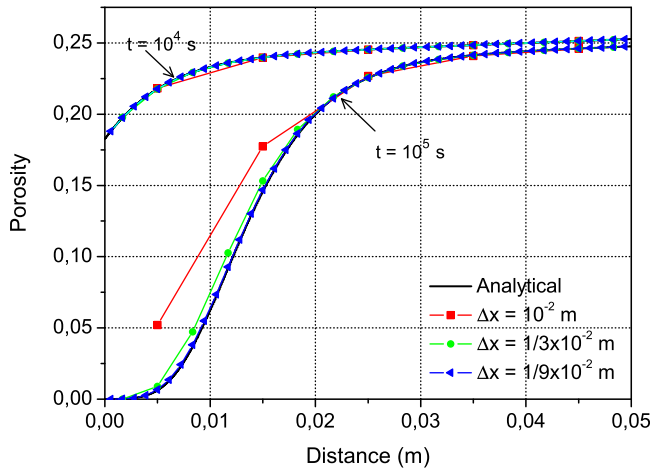
Figure 8. The analytical and numerical solutions of the porosity for different mesh sizes at times 10^4 and 10^5 s.

[38] It is important to mention that by changing the parameters of the governing equations, such as the initial concentration and/or the function $f(x)$, the same analytical solutions can be used to describe different problems of precipitation and/or dissolution (decrease and/or increase in porosity). For problems involving precipitation, $f(x)$ should be chosen in such a way that $f(x)c(x,t) > K$. In the case of dissolution, the function $f(x)$ must verify $f(x)c(x,t) < K$. The objective of the examples was to show the validity of the analytical solutions when the reaction causes strong change in the porosity. As we can observe in Figures 2 and 6, the gradient of the porosity $\partial\phi/\partial x$ at the front goes to infinity with time. To obtain an approximate solution to the system (7), *Lagneau and van der Lee* [2010] neglected the term $\partial\phi/\partial x$. This limits the applicability of their solutions to the very beginning of the porosity evolution. In contrast, the solutions obtained in this work are valid for arbitrary strong change in porosity.

6. Comparison With Numerical Solutions

[39] We use the analytical solutions to validate numerical solutions of system (7). A global implicit finite volume scheme is used to integrate the equations numerically.
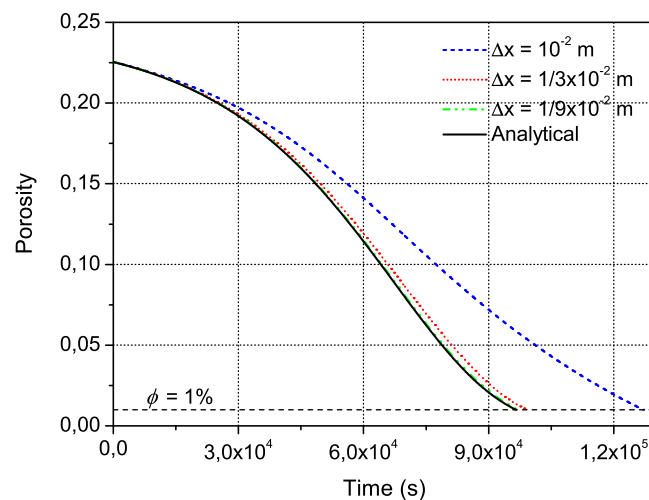
[40] In addition to the analytical solutions, we plot in Figures 1–4 the numerical solutions at different times for the problem of mineral precipitation studied in section 5. These solutions reproduce the solute concentrations, the porosities, and the solid concentrations. For the numerical solutions, we have used 50 evenly spaced elements (which corresponds to a mesh size of 10^{-3} m), and the time step is fixed to 1 s. As compared in Figures 1–4, the analytical solutions can be considered to be identical to the numerical solutions even though the analytical solutions require much less CPU time.

[41] In order to investigate the effect of spatial discretizations, three additional calculations were performed with mesh sizes $\Delta x = 10^{-2}$, $\frac{1}{3} \times 10^{-2}$ and $\frac{1}{9} \times 10^{-2}$ m. Figure 8 shows the analytical porosity profiles as well as the numerical solutions at two different times: $t = 10^4$ s (at the beginning of the porosity decrease) and $t = 10^5$ s (near clogging). For $t = 10^4$ s, the numerical solutions are close to the analytical solution independently of the mesh size. However, we observe some differences for $t = 10^5$ s. Figure 9 shows the temporal evolution of the porosity at location $x = 5 \times 10^{-3}$ m for the three spatial discretizations. A porosity of 1% is reached after 127,100 s for $\Delta x = 10^{-2}$, $t_c = 99,200$ for $\Delta x = \frac{1}{3} \times 10^{-2}$, and $t_c = 97,000$ s for $\Delta x = \frac{1}{9} \times 10^{-2}$. The exact time (calculated from equation (49)) necessary for the porosity to reach 1% at location $x = 5 \times 10^{-3}$ m is $t_c = 96,543$ s. We observe that the numerical solution converges to the analytical solution when Δx is small enough to resolve the concentration front.

[42] *Marty et al.* [2009] provided detailed numerical investigations of clogging at concrete-clay interfaces in a diffusive transport regime. They found that for an equilibrium chemistry approach (fast kinetics) the calculated clogging time depends strongly on the spatial discretization of the numerical integration scheme. The numerical solution confirms that the clogging times in the case of equilibrium chemistry will converge to zero. In this case the precipitation of minerals and the connected porosity change are completely controlled by the diffusive flux of reacting solutes toward the numerical nodes. For a given diffusive flux, porosity changes in a numerical nodes will depend on the volume of the numerical node, which is directly related to the spatial discretization. In addition, in more complex chemical

Figure 9. The temporal evolution of the porosity at location $x = 5 \times 10^{-3}$ m for different mesh sizes.

systems, different mineral equilibria at neighboring nodes define different solute concentrations at neighboring nodes. For such situations, diffusive fluxes between neighboring nodes depend on node distances too. Therefore, a decrease in node distance (refinement of grid size) will increase diffusive fluxes and at the same time increase the volume fraction filled by the precipitate. Our analytical solutions are only suitable for nonequilibrium chemistry (i.e., kinetic control of precipitation reactions). Like *Marty et al.* [2009], we observe a convergence of the numerical clogging time toward a constant value for finer spatial discretizations. With increasing kinetic control of precipitation reactions, specific equilibrium concentrations at neighboring nodes are suppressed, and spatial concentration gradients develop. Correct numerical solutions are only obtained if the numerical grids resolve these concentration gradients sufficiently.

[43] *Lagneau and van der Lee* [2010] stated that only an implicit scheme produces accurate solutions for any time step size on the basis of their comparison between numerical and analytical solutions for reactive transport with moderate porosity changes. Our experience confirms this, as test calculations with an explicit scheme did not always converge to the analytical solution.

7.   Conclusion

[44] In this paper, we derived analytical solutions for a one-dimensional coupled diffusion-reaction problem with feedback of porosity change by using the simplest equation method. The proposed analytical solutions are exact, explicit in space and time variables, and do not contain any approximation. These analytical solutions contain a number of arbitrary functions, which offer a framework for deriving more closed form solutions under various initial and boundary conditions. These analytical solutions can be used for benchmarking numerical codes, as shown in the presented example. We obtained a good agreement between numerical and analytical solutions when a sufficient spatial discretization is used, which resolves the spatial concentration gradients at any time. It is important to mention that the solutions proposed here are limited to two-component systems where one component is stationary. This is probably a case rarely found in natural systems. Therefore, further work to describe multicomponent systems is needed in order to develop more realistic analytical benchmarks.

Appendix A: The Simplest Equation Method

[45] The simplest equation method provides an analytical solution for nonlinear ordinary differential equations in the form

$$P\left(y, \frac{\mathrm{d}y}{\mathrm{d}\xi}, \frac{\mathrm{d}^2 y}{\mathrm{d}\xi^2}, y\frac{\mathrm{d}y}{\mathrm{d}\xi}, \dots\right), \tag{A1}$$

where P is a polynomial in the unknown variable $y = y(\xi)$ and its derivatives. The idea of this method is to assume that the solution of equation (A1) can be expanded in finite series of the form

$$y(\xi) = \sum_{k=0}^{N} A_k Y^k, A_N \neq 0, \tag{A2}$$

where coefficients A_k are independent of ξ, which is to be determined, N is an integer to be determined, and $Y = Y(\xi)$ is a function that verifies some ordinary differential equation. This ordinary differential equation is called the simplest equation. The order of the admissible simplest equation is less than that of equation (A1). In order to express the exact solutions $y(\xi)$ of equation (A1) as finite series (A2), the general solution $Y = Y(\xi)$ of the chosen simplest equation has to be known.

[46] In this work, we use the Bernoulli equation as the simplest equation

$$\frac{\mathrm{d}Y}{\mathrm{d}\xi} = aY + bY^2, \tag{A3}$$

which has general solutions of the form

$$Y(\xi) = \frac{a\exp[a(\xi + \xi_0)]}{1 - b\exp[a(\xi + \xi_0)]} \tag{A4}$$

when $b \neq 0$ and

$$Y(\xi) = \exp[a(\xi + \xi_0)] \tag{A5}$$

when $b = 0$, where ξ_0 is a constant of integration.

Appendix B: Derivation of the Porosity Functions

[47] The porosity function is calculated by using equation (20). Substituting (22) into (20) yields

$$\Phi(\xi) = \Phi_1 \exp\left(-\frac{kS_0 V_m}{\lambda K}\left\{[K - f(x)A_0(x)](\xi - \xi_1)\right. \right.$$
$$\left.\left. - f(x)A_1(x)\int_{\xi_1}^{\xi} Y(\xi')\mathrm{d}\xi'\right\}\right). \tag{B1}$$

[48] The integral $\int_{\xi_1}^{\xi} Y(\xi')\mathrm{d}\xi'$ depends on the solution of the Bernoulli equation (A3). If solution (A4) is used, we obtain

$$\int_{\xi_1}^{\xi} Y(\xi')\mathrm{d}\xi' = \int_{\xi_1}^{\xi} \frac{a(x)\exp[a(x)(\xi' + \xi_0)]}{1 - b(x)\exp[a(x)(\xi' + \xi_0)]}$$
$$\mathrm{d}\xi' = -\frac{1}{b(x)}\ln\left|\frac{1 - b(x)\exp[a(x)(\xi + \xi_0)]}{1 - b(x)\exp[a(x)(\xi_1 + \xi_0)]}\right|. \tag{B2}$$

In this case, equation (B1) becomes

$$\begin{aligned}
\Phi(\xi) &= \Phi_1 \exp\left(-\frac{kS_0 V_m}{\lambda K}\left\{[K - f(x)A_0(x)](\xi - \xi_1) + \frac{f(x)A_1(x)}{b(x)}\ln\left|\frac{1 - b(x)\exp[a(x)(\xi + \xi_0)]}{1 - b(x)\exp[a(x)(\xi_1 + \xi_0)]}\right|\right\}\right). \\
&= \Phi_1 \exp\left\{-\frac{kS_0 V_m[K - f(x)A_0(x)]}{\lambda K}(\xi - \xi_1)\right\}\left|\frac{1 - b(x)\exp[a(x)(\xi + \xi_0)]}{1 - b(x)\exp[a(x)(\xi_1 + \xi_0)]}\right|^{-\frac{kS_0 V_m f(x)A_1(x)}{\lambda Kb(x)}}.
\end{aligned} \tag{B3}$$

However, if solution (A5) is used, then

$$
\int_{\xi_1}^{\xi} Y(\xi')\mathrm{d}\xi' = \int_{\xi_1}^{\xi} a(x)\exp[a(\xi' + \xi_0)]\mathrm{d}\xi'
$$

$$
= \frac{\exp[a(x)(\xi + \xi_0)] - \exp[a(x)(\xi_1 + \xi_0)]}{a(x)}. \tag{B4}
$$

In this case, equation (B1) becomes

$$
\Phi(\xi) = \Phi_1 \exp\left\{ -\frac{kS_0 V_m}{\lambda K}[K - f(x)A_0(x)](\xi - \xi_1)\right\}
$$

$$
+ \exp\left(\frac{kS_0 V_m f(x)A_1(x)}{\lambda K a(x)}\{\exp[a(x)(\xi + \xi_0)]\right. \tag{B5}
$$

$$
\left. - \exp[a(x)(\xi_1 + \xi_0)]\}\right).
$$

References

Adler, M., U. K. Mäder, and H. N. Waber (1998), Experiment vs. modelling: Diffusive and advective interaction of high-pH solution in argillaceous rock at 35°C, *Mineral. Mag.*, *62*, 15–16.

Amos, R., and K. Mayer (2006), Investigating the role of gas bubble formation and entrapment in contaminated aquifers: Reactive transport modelling, *J. Contam. Hydrol.*, *87*, 123–154.

Bear, J. (1972), *Dynamics of Fluids in Porous Media*, Dover, New York.

Boving, T. V., and P. Grathwohl (2001), Tracer diffusion coefficients in sedimentary rocks: Correlation to porosity and hydraulic conductivity, *J. Contam. Hydrol.*, *53*, 85–100.

Burnol, A., P. Blanc, T. Xu, N. Spycher, and E. C. Gaucher (2006), Uncertainty in the reactive transport model response to an alkaline perturbation in a clay formation, In *Proceedings, TOUGH Symposium 2006*, Lawrence Berkeley Natl. Lab., Berkeley, Calif. [Available at http://esd.lbl.gov/TOUGH+/proceedings-2006.html]

Charlet, L., S. Chakraborty, C. A. J. Appelo, G. Roman-Ross, B. Nath, A. A. Ansari, M. Lanson, D. Chatterjee, and S. Basu Mallik (2007), Chemodynamics of an arsenic hotspot in a West Bengal aquifer: A field and reactive transport modeling study, *Appl. Geochem.*, *22*, 1273–1292.

Cussler, E. L. (1982), Dissolution and reprecipitation in porous solids, *AIChE J.*, *28*, 500–508.

Cussler, E. L., J. Kopinsky, and J. A. Weimer (1983), The effect of pore diffusion on the dissolution of porous mixtures, *Chem. Eng. Sci.*, *38*, 2027–2033.

Desaulniers, D. E., J. A. Cherry, and P. Fritz (1981), Age and movement of pore water in argillaceous quaternary deposits at four sites in southwestern Ontario, *J. Hydrol.*, *50*, 231–257.

De Windt, L., H. Schneider, C. Ferry, H. Catalette, V. Lagneau, C. Poinssot, A. Poulesquen, and C. Jegou (2006), Modeling radionuclide source-terms and release in a spent nuclear fuel disposal, *Radiochim. Acta*, *94*, 787–794.

De Windt, L., D. Pellegrini, and J. van der Lee (2007a), Coupled modeling of cement/claystone interactions and radionuclide migration, *J. Contam. Hydrol.*, *68*, 165–182.

De Windt, L., R. Badreddine, and V. Lagneau (2007b), Long-term reactive transport modelling of stabilised/solidified waste: From dynamic leaching tests to disposal scenarios, *J. Hazard. Mater.*, *139*, 529–536.

Gaucher, E. C., E. Blanc, J. M. Matray, and N. Michau (2004), Modelling diffusion of an alkaline plume in a clay barrier, *Appl. Geochem.*, *19*, 1505–1515.

Gruber, J. (1990), Containment accumulation during transport through porous media, *Water Resour. Res.*, *26*, 99–107, doi:10.1029/WR026i001p00099.

Helfferich, F., and A. Katchalsky (1970), A simple model of interdiffusion with precipitation, *J. Phys. Chem.*, *74*, 308–314.

Jang, Y. S., and Y. I. Kim (2003), Behavior of a municipal landfill from field measurement data during a waste-disposal period, *Environ. Geol.*, *44*, 592–598.

Johnson, R. L., J. A. Cherry, and J. F. Pankow (1989), Diffusive contaminant transport in natural clay: A field example and implications for clay-lined waste disposal sites, *Environ. Sci. Technol.*, *23*, 340–349.

Knabner, P., C. J. van Duijn, and S. Hengst (1995), An analysis of crystal dissolution fronts in flows through porous media. Part 1: Compatible boundary conditions, *Adv. Water Resour.*, *18*, 171–185.

Kudryashov, N. A. (2005a), Simplest equation method to look for exact solutions of nonlinear differential equations, *Chaos Solitons Fractals*, *24*, 1217–1231.

Kudryashov, N. A. (2005b), Exact solitary waves of the Fisher equation, *Phys. Lett. A*, *342*, 99–106.

Kudryashov, N. A., and N. B. Loguinova (2008), Extended simplest equation method for nonlinear differential equations, *Appl. Math. Comput.*, *205*, 396–402.

Lagneau, V., and J. van der Lee (2010), Operator-splitting-based reactive transport models in strong feedback of porosity change: The contribution of analytical solutions for accuracy validation and estimator improvement, *J. Contam. Hydrol.*, *112*, 118–129.

Landais, P. (2004), Clays in natural and engineered barriers for radioactive waste confinement, *Appl. Clay Sci.*, *26*, 1.

Lichtner, P. C. (1991), The quasi-stationary state approximation to fluid/rock reactions: Local equilibrium revisited, in *Diffusion, Atomic Ordering, and Mass Transport*, edited by J. Ganguly, pp. 452–560, Springer, Berlin.

Lichtner, P. C. (1996), Continuum formulation of multicomponent-multiphase reactive transport, in *Reactive Transport in Porous Media, Rev. Mineral.*, vol. 34, edited by P. C. Lichtner, C. I. Steefel, and E. H. Oelkers, pp. 1–81, Mineral. Soc. of Am, Washington, D. C.

Lichtner, P. C., E. H. Oelkers, and H. C. Helgeson (1986a), Interdiffusion with multiple precipitation/dissolution reactions: Transient model and steady-state limit, *Geochim. Cosmochim. Acta*, *50*, 1951–1966.

Lichtner, P. C., E. H. Oelkers, and H. C. Helgeson (1986b), Exact and numerical solutions to the moving boundary problem resulting from reversible heterogeneous reactions and aqueous diffusion in a porous medium, *J. Geophys. Res.*, *91*, 7531–7544.

Liu, C., and W. P. Ball (1998), Analytical modeling of diffusion-limited contamination and decontamination in a two-layer porous medium, *Adv. Water Resour.*, *21*, 297–313.

MacQuarries, K. T. B., and K. U. Mayer (2005), Reactive transport modeling in fractured rock: A state-of-the-science review, *Earth Sci. Rev.*, *72*, 189–227.

Marty, N. C. M., C. Tournassat, A. Burnol, E. Giffaut, and E. C. Gaucher (2009), Influence of reaction kinetics and mesh refinement on the numerical modelling of concrete/clay interactions, *J. Hydrol.*, *364*, 58–72.

Navarro, J. A. S., C. Lopez, and A. P. Garcia (2000), Characterization of groundwater flow in the Bailin hazardous waste-disposal site (Huesca, Spain), *Environ. Geol.*, *40*, 216–222.

Noiriel, C., P. Gouze, and D. Bernard (2004), Investigation of porosity and permeability effects from microstructure changes during limestone dissolution, *Geophys. Res. Lett.*, *31*, L24603, doi:10.1029/2004GL021572.

Noiriel, C., B. Madé, and P. Gouze (2007), Impact of coating development on the hydraulic and transport properties in argillaceous limestone fracture, *Water Resour. Res.*, *43*, W09406, doi:10.1029/2006WR005379.

Ortoleva, P., E. Merino, C. Moore, and J. Chadam (1987a), Geochemical self-organization, I. Reaction-transport feedback and modeling approach, *Am. J. Sci.*, *287*, 979–1007.

Ortoleva, P., J. Chadam, E. Merino, and A. Sen (1987b), Geochemical self-organization, II. The reactive-infiltration instability, *Am. J. Sci.*, *287*, 1008–1040.

Piantone, P., C. Nowak, P. Blanc, A. Lassin, and A. Burnol (2006), THE-MODDEM: Thermodynamique et Modélisation de la Dégradation Déchets Minéraux, rapport d'avancement, *Rep. BRGM/RP-54547-FR*, Bur. de Rech. Géol. et Min., Orléans, France.

Polyanin, A. D., and V. F. Zaitsev (2003), *Handbook of Exact Solutions for Ordinary Differential Equations*, 2nd ed., 787 pp., Chapman and Hall/CRC, Boca Raton, Fla.

Saripalli, K. P., P. D. Meyer, D. H. Bacon, and V. L. Freedman (2001), Changes in hydrologic properties of aquifer media due to chemical reactions: A review, *Crit. Rev. Environ. Sci. Technol.*, *31*, 311–349.

Savage, D., D. Noy, and M. Mihara (2002), Modelling the interaction of bentonite with hyperalkaline fluids, *Appl. Geochem.*, *17*, 207–223.

Shackelford, C. D., and D. E. Daniel (1991), Diffusion in saturated soil. I: Background, *J. Geotech. Eng.*, *117*, 467–484.

Singurindy, O., and B. Berkowitz (2003a), Evolution of hydraulic conductivity by precipitation and dissolution in carbonate rock, *Water Resour. Res.*, *39*(1), 1016, doi:10.1029/2001WR001055.

Singurindy, O., and B. Berkowitz (2003b), Flow, dissolution, and precipitation in dolomite, *Water Resour. Res.*, *39*(6), 1143, doi:10.1029/2002WR001624.

Soler, J. M. (2003), Reactive transport modeling of the interaction between a high-pH plume and a fractured marl: The case of Wellenberg, *Appl. Geochem.*, *18*, 1555–1571.

Spiteri, C., C. P. Slomp, P. Regnier, C. Meile, and P. Van Cappellen (2007), Modelling the geochemical fate and transport of wastewater-derived phosphorus in contrasting groundwater systems, *J. Contam. Hydrol.*, *92*, 87–108.

Steefel, C. I., and P. C. Lichtner (1994), Diffusion and reaction in rock matrix bordering a hyperalkaline fluid-filled fracture, *Geochim. Cosmochim. Acta*, *58*, 3595–3612.

Steefel, C. I., and P. C. Lichtner (1998), Multicomponent reactive transport in discrete fractures II: Infiltration of hyperalkaline groundwater at Maqarin, Jordan, a natural analogue site, *J. Hydrol.*, *209*, 200–224.

Steefel, C. I., and K. Maher (2009), Fluid-rock interaction: A reactive transport approach, *Rev. Mineral. Geochem.*, *70*, 485–532.

Trotignon, L., H. Peycelon, and X. Bourbon (2006), Comparison of performance of concrete barriers in a clayey geological medium, *Phys. Chem. Earth.*, *31*, 610–617.

Trotignon, L., V. Devallois, H. Peycelon, C. Tiffreau, and X. Bourbon (2007), Predicting the long term durability of concrete engineered barriers in a geological repository for radioactive waste, *Phys. Chem. Earth.*, *32*, 259–274.

van Duijn, C. J., P. Knabner, and R. J. Schotting (1998), An analysis of crystal dissolution fronts in flows through porous media, part 2: Incompatible boundary conditions, *Adv. Water Resour.*, *22*, 1–16.

Vieillard, P., S. Ramirez, A. Bouchet, A. Cassagnabere, A. Meunier, and E. Jacquot (2007), Alteration of the Callovo-Oxfordian clay from Meuse-Haute Marne Underground Laboratory (France) by alkaline solution: II. Modelling of mineral reactions, *Appl. Geochem.*, *19*, 1699–1709.

Vitanov, N. K., and Z. I. Dimitrova (2010), Application of the method of simplest equation for obtaining exact traveling-wave solutions for two classes of model PDEs from ecology and population dynamics, *Commun. Nonlinear. Sci. Numer. Simul.*, *15*, 2836–2845.

Vitanov, N. K., Z. I. Dimitrova, and H. Kantz (2010), Modified method of simplest equation and its application to nonlinear PDEs, *Appl. Math. Comput.*, *216*, 2587–2595.

Weare, J. H., J. R. Stephens, and H. P. Eugster (1976), Diffusion matasomatism and mineral reaction zones: General principles and application to feldspar alteration, *Am. J. Sci.*, *276*, 767–816.

S. Churakov, M. Hayek, and G. Kosakowski, Laboratory for Waste Management, Paul Scherrer Institut, CH-5232 Villigen PSI, Switzerland. (mohamed.hayek@gmail.com)